LINCOLN LABORATORY

G -

A MECHANICALLY FIXED RADAR ANTENNA WITH SCANNING CAPABILITY

For a radar antenna system that scans a region of space subtending a small angle at the antenna, the generally adopted mechanism utilizes a fixed paraboloid and a mobile feed horn. It was suggested that a stationary feed system consisting of more than one radiation source should have advantages not otherwise available.

1. There would be no mechanical limitations. All scanning would be accomplished electrically.
2. The maximum power that can be radiated depends on the power handling capability of the components in the radiation feed system. With a multiple feed assembly, higher beam powers can be readily obtained.
3. There should be less deterioration of the antenna beam when it scans off boresight since the phase and amplitude of the sources can be adjusted to tend to correct any phase errors of the wave front after reflection from the paraboloid.

Desirable qualities of such a system are:

1. As many as possible of the radiation sources are excited to maximum, or near maximum, power for any of the possible beam directions in any scanning operation.
2. There should be a minimum number of sources and yet retain good antenna characteristics.
3. The sources should present minimum aperture block, thus limiting the area that they may cover.

In particular, an antenna system with cylindrical symmetry was analyzed because the 3-dimensional problem reduces to one of two dimensions and simplifies

the mathematics. The geometry is shown in Figure 1. The focal length f of the reflector, a parabolic cylinder, and its aperture width 2a were set equal to 30λ and 60λ respectively. This was illuminated by an array of line sources located in a plane normal to the focal plane of the parabolic cylinder and a distance R from the vertex. Each line source, located a distance σ from the focal plane, was assumed to be a horn having a radiation pattern in the plane of the parabola given by the gain function $g(\alpha) = \cos^2\alpha$. This was chosen because it approximated the pattern of an open ended waveguide.

Since the study is primarily one of feasibility and quantitative values are less important, various approximations for the purpose of simplification were devised.

1. The 2-dimensional problem was solved.
2. Scalar wave theory was used.
3. The picture was idealized so that only that radiation emanating from the source, reflected once and then traveling undisturbed to the point of observation contributes to the calculated field. Thus, aperture block was neglected.
4. Rim currents were not introduced to match boundary conditions.

The equations that characterize the patterns are developed in the latter part of this paper and the IBM 7090 computer was used for all calculations. To obtain the quantitative results, the following procedure was used:

1. A plane wave was assumed incident on the antenna. θ_o, the angle between the direction of propagation of the plane wave and the axis of the parabola (boresight) was set at 3 values, 0°, 4° and 8°. Since the expected beamwidth is approximately 1° this constitutes a scan limit of $\pm$ 8 beamwidths.

2. The relative amplitude of the signal received by a horn, u_p, was calculated for all combinations of the 8 values of R = 20λ, 21λ, 22λ, 23λ, 24λ, 25λ, 26λ, 27λ, and the 21 values of σ = -6.0λ, -5.4λ, -4.8λ, - - - - - +5.4λ, +6.0λ. It was expected that the R chosen in a final design would fall in this range, and because of aperture block, σ is limited to a maximum of 1/5 a.
3. The horn was converted to a transmitter radiating a signal u_p^*, the complex conjugate of u_p.
4. The far field u_Q was then found over a range of θ. θ is the angle that a line in the direction of Q, the field point, makes with the axis of the parabola.
5. For several horns radiating simultaneously, the field at Q is the sum of fields produced by each horn radiating alone. For each R, the field pattern was then found for 21 radiating horns covering the 21 values of σ.

Figures 2 to 9 are graphs of these patterns showing the relative amplitude, in decibels, versus the angle θ for R = 20λ to 27λ. Each figure has 3 patterns for $\theta_o = 0^o$, 4^o and 8^o and each pattern has a graph insert showing the horn position σ, and relative amplitude $|u|$ of the signals that produced it.

Figures 10, 11 and 12 summarize the main characteristics as a function of R. Figure 10 is the gain, Figure 11 is the beamwidth at the 3 db and 10 db levels and Figure 12 is the side lobe level for the highest left and right side lobes. There is no distinct side lobe structure for $\theta_o = 8^o$. Included in these figures are the characteristics that a single horn located at the focus of the parabola would produce.

It is apparent that the patterns deteriorate as R decreases. On the other hand, the source amplitude distributions are less desirable for the higher R values. It appears that R = 24λ is a good compromise.

The final consideration is the effect of altering the number of horns. The procedure layed out above was repeated for R = 24λ and various sets of values of σ.

Figure 13: 31 horns separated .4λ, σ = -6.0λ, -5.6λ, -5.2λ ----+6.0λ.

Figure 14: 21 horns separated .6λ, σ = -6.0λ, -5.4λ, -4.8λ ----+6.0λ.

Figure 15: 16 horns separated .8λ, σ = -6.0λ, -5.2λ, -4.4λ ----+6.0λ.

Figure 16: 13 horns separated 1.0λ, σ = -6.0λ, -5.0λ, -4.0λ ----+6.0λ.

Figure 17: 11 horns separated 1.2λ, σ = -6.0λ, -4.8λ, -3.6λ ----+6.0λ.

The interesting feature is that for 16 or fewer horns, the side lobe level is unusually high - less than 12 db - and 21 horns effects a considerable decrease in side-lobe level - to more than 18 db. For this reason, it appears that more than 16 horns are required to produce a good antenna pattern.

In view of the results of this analysis, there appears to be merit in this type of antenna system. If a paraboloid type reflector is to be considered, the solution of the 3-dimensional problem would provide more accurate quantitative values. It should be realized, of course, that any scanning mechanism that extends beyond a simple plane would require a more elaborate system of horns than a single row.

A theoretical development of the equations used follows so as to enable the curious reader to examine in greater detail, the assumptions made and physical reasoning applied.

The antenna system is represented in Figure 1. The reflector has a parabolic cross section and the group of horns lies normal to the axis of the parabola near its focus. Two isotropic units, A and B, are located in the "far field" of the antenna. If A is radiating and B is not, and if the horns receive all the energy that is reflected from the parabola, then the principle of reciprocity indicates that if the situation is altered to having the horns transmit signals whose values are the complex conjugate of the signals they received, A receives all the energy and B receives none. (It is assumed that no energy coupling exists between any two horns or between A and B.) This is the ideal condition for this result holds true regardless of the position of B and the radiation pattern must then apprcach a Dirac delta function whose peak lies at A.

In a practical situation, all the energy radiated by A and reflected would not be received by the horn array, and fewer horns are more desirable. In addition, it is difficult to tell whether the phase or amplitude of one signal should be changed to improve the pattern if the array geometry is changed. But the principle of reciprocity can be used to compute a signal for each horn to radiate knowing that increasing the number of horns, the pattern characteristics improves.

The scalar field, u, at a point in a region satisfies the wave equation $\nabla^2 u + k^2 u = 0$, $k = \frac{2\pi}{\lambda}$. In the 3-dimensional case, this equation has the solution

$$4\pi u_p = \int_A \left(u \frac{\partial v}{\partial n} - v \frac{\partial u}{\partial n} \right) dA$$

where the integration is over the boundary of the region.

u_p is the field at the point, p, inside the region.

u is the field on the boundary.

n is the normal to the boundary directed into the region.

$v = \frac{e^{ikr}}{r}$, r is the distance from p to the boundary.

In the 2-dimensional problem, the integral becomes

$$-4iu_p = \int_\Gamma \left(u \frac{\partial v}{\partial n} - v \frac{\partial u}{\partial n} \right) d\Gamma \qquad (1)$$

where the integration is over the closed curve, Γ

u_p, u, n have the same meaning.

And in the numerical calculations, the v used was again*

$$v = \frac{e^{ikr}}{r}$$

A plane wave illuminates the parabola and thus

$$u = e^{-iks}$$

s is the distance from the plane wave to a point on the parabola measured along the direction of propagation of the plane wave. The plane wave is located so that s = 0 at the vertex of the parabola.

* After the calculations were performed, it was realized that this form of v was not correct. For values of $kr > 100$, as is the case here, the v should be taken as $\frac{e^{ikr}}{r^{1/2}}$. To check the effect of using this formula for v, the calculations were repeated for Figure 6, and the patterns altered very slightly, a change that one would say is equivalent to a very small change in the horn characteristic pattern.

Substituting for u and v in equation (1) and simplifying,

$$u_p = \left(\frac{k^3 R}{8\pi}\right)^{1/2} \int_\Gamma g(\alpha) \frac{e^{ik(r-s)}}{kr}$$

$$\left[\left(1 - \frac{1}{ikr}\right) \cos(r, n) + \cos(s, n)\right] d\Gamma \qquad (2)$$

(r, n) and (s, n) are the angles between the directions of r and n and s and n respectively. $g(\alpha)$ is introduced to characterize the horns which are not isotropic. $g(\alpha)$ is the horn gain at angle, α.

To determine the far field, u_Q, the same formula (1) is used. The horn radiates a signal, u_p^*, the complex conjugate of u_p and the parabola is then illuminated by a signal $u = g(\alpha) \frac{e^{ikr}}{kr} u_p^*$.

Also,

$$v = \left(\frac{2}{\pi k D}\right)^{1/2} e^{ikD - iks}$$

D-s is the distance from the far-field point to the parabola. D is a constant, s goes to 0 at the parabola vertex.

Substituting and simplifying,

$$u_Q = \left(\frac{k}{8\pi D}\right)^{1/2} e^{ikD} u_p^*$$

$$\int_\Gamma g(\alpha) \frac{e^{ik(r-s)}}{kr} \left[\left(1 - \frac{1}{ikr}\right) \cos(r, n) + \cos(s, n)\right] d\Gamma \qquad (3)$$

(2) and (3) are the equations to be solved. In both formulas, Γ is the contour of the parabola and is given by the equation $x = \frac{y^2}{4f}$.

The normal $\vec{n}$ is a vector $\frac{i\,dy - j\,dx}{(dx^2 + dy^2)^{1/2}} = \frac{i\,dy - j\,dx}{d\Gamma}$

i and j are the unit vectors along the X and Y axes.

(R, σ) are the coordinates of p

$$\vec{r} = i\,(R - x) + j\,(\sigma - y)$$

$$r = \left[(R - x)^2 + (\sigma - y)^2\right]^{1/2}$$

$$\vec{s} = (i \cos\theta + j \sin\theta)\, s$$

$$s = x \cos\theta + y \sin\theta$$

$$\cos(r, n) = \frac{\vec{r} \cdot \vec{n}}{r} = \frac{(R - x)\,dy - (\sigma - y)\,dx}{r\,d\Gamma}$$

$$= \frac{1}{r}\left[R - x - (\sigma - y)\frac{dx}{dy}\right]\frac{dy}{d\Gamma}$$

$$\cos(s, n) = \frac{\vec{s} \cdot \vec{n}}{s} = \frac{\cos\theta\,dy - \sin\theta\,dx}{d\Gamma}$$

$$= \left(\cos\theta - \sin\theta\frac{dx}{dy}\right)\frac{dy}{d\Gamma}$$

The $\frac{dy}{d\Gamma}$ in the two expressions will combine with the $d\Gamma$ in the integral to convert to an integration over y from y = -a to y = + a, the extent of the parabola. Finally, $\cos\alpha = \frac{R - x}{r}$ provides the value for $g(\alpha) = \cos^2\alpha$. Thus, the necessary equations have been derived.

CAPTIONS

Figure 1: A schematic representation of the antenna system.

Figure 2: The far-field patterns calculated for $R = 20\lambda$, $\theta_o = 0^\circ$, 4° and 8°. 21 horns separated $.6\lambda$, $\sigma = -6.0\lambda, -5.4\lambda, -4.8\lambda$ ---- $+6.0\lambda$. Each pattern has a graph insert showing the horn position σ and horn relative signal amplitude $|u|$.

Figure 3: $R = 21\lambda$

Figure 4: $R = 22\lambda$

Figure 5: $R = 23\lambda$

Figure 6: $R = 24\lambda$

Figure 7: $R = 25\lambda$

Figure 8: $R = 26\lambda$

Figure 9: $R = 27\lambda$

Figure 10: The calculated gain as a function of R. The dashed line is the value that a single horn located at the focus would have.

Figure 11: The beamwidth at the 3 db and 10 db levels.

Figure 12: The side lobe level of the highest left and right-side lobes.

Figure 13: The far-field patterns calculated for $R = 24\lambda$, $\theta_o = 0^\circ$, 4° and 8°. 31 horns separated $.4\lambda$, $\sigma = -6.0\lambda, -5.6\lambda, -5.2\lambda$ ---- $+6.0\lambda$. Each pattern has a graph insert showing the horn position σ and horn relative signal amplitude $|u|$.

Figure 14: 21 horns separated $.6\lambda$, $\sigma = -6.0\lambda, -5.4\lambda, -4.8\lambda$ ---- $+6.0\lambda$.

Figure 15: 16 horns separated $.8\lambda$, $\sigma = -6.0\lambda, -5.2\lambda, -4.4\lambda$ ---- $+6.0\lambda$.

Figure 16: 13 horns separated 1.0λ, $\sigma = -6.0\lambda, -5.0\lambda, -4.0\lambda$ ---- $+6.0\lambda$.

Figure 17: 11 horns separated 1.2λ, $\sigma = -6.0\lambda, -4.8\lambda, -3.6\lambda$ ---- $+6.0\lambda$.

Figure 1: A schematic representation of the antenna system.

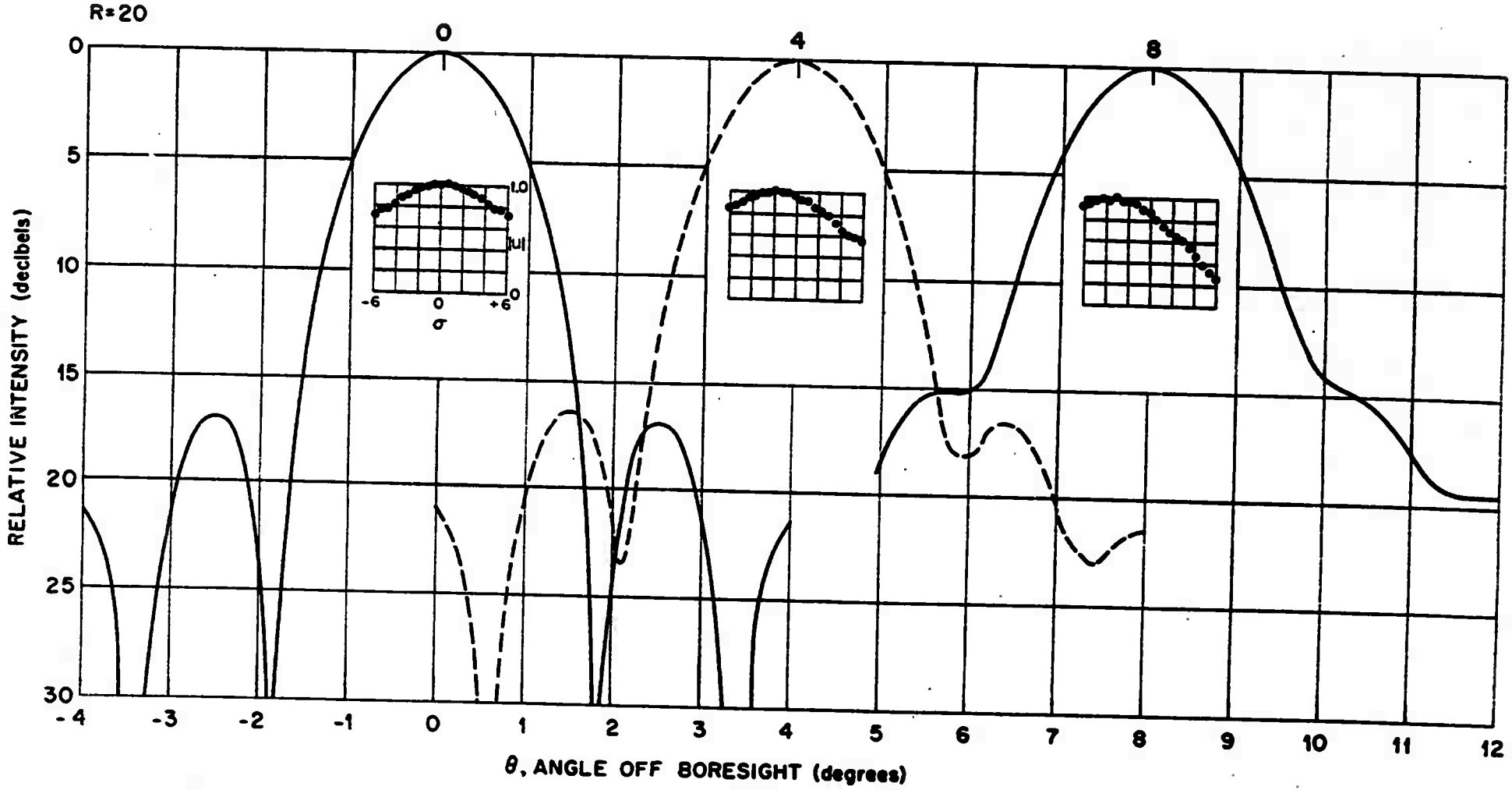

Figure 2: The far-field patterns calculated for R = 20λ, Θ_o = 0°, 4° and 8°. 21 horns separated .6λ, σ = -6.0λ, -5.4λ, -4.8λ ---- +6.0λ. Each pattern has a graph insert showing the horn position σ and horn relative signal amplitude u .

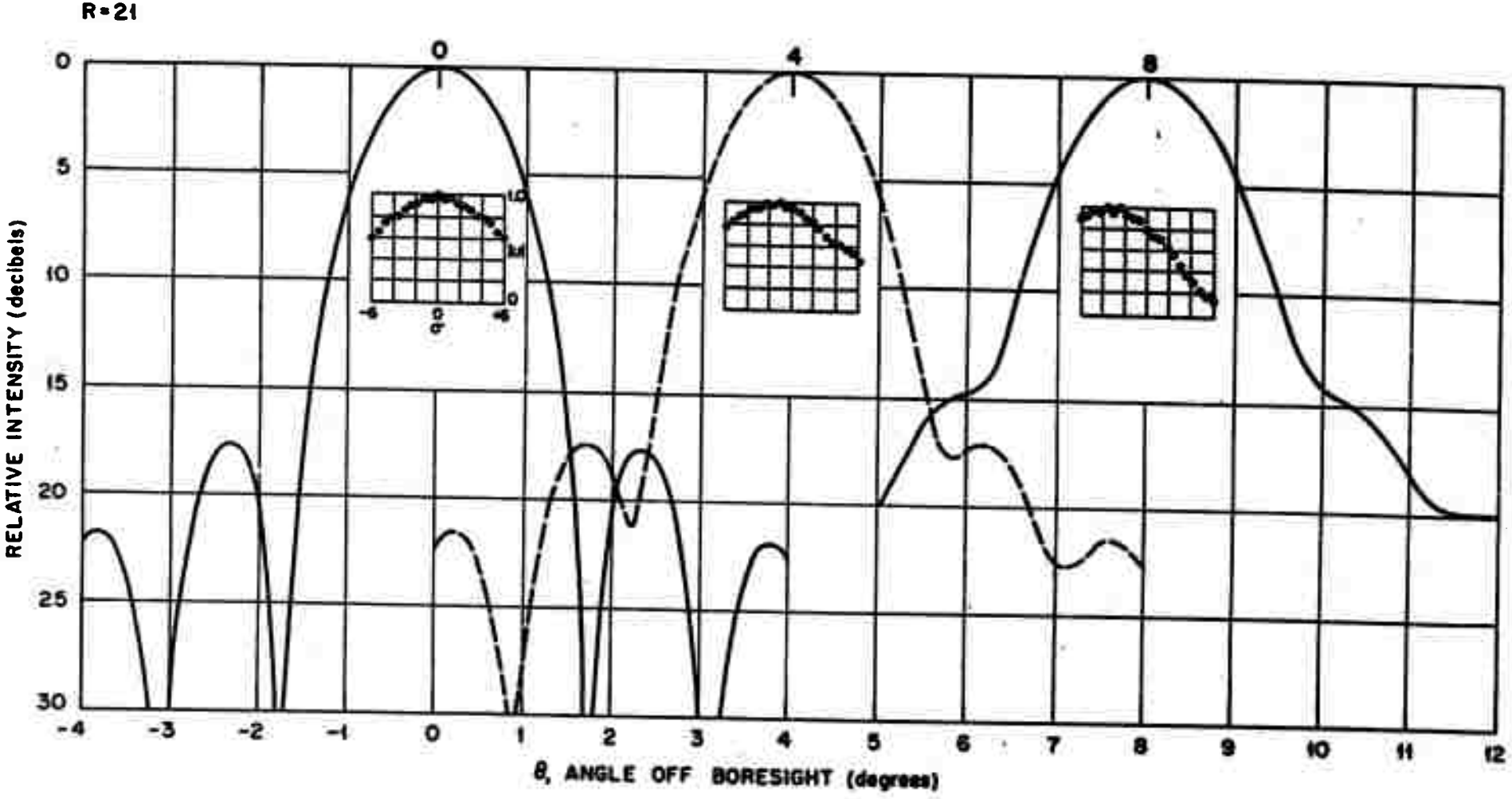
R=21
0
4
8
RELATIVE INTENSITY (decibels)
0
5
10
15
20
25
30
-4
-3
-2
-1
0
1
2
3
4
5
6
7
8
9
10
11
12
θ, ANGLE OFF BORESIGHT (degrees)

Figure 3: R = 21

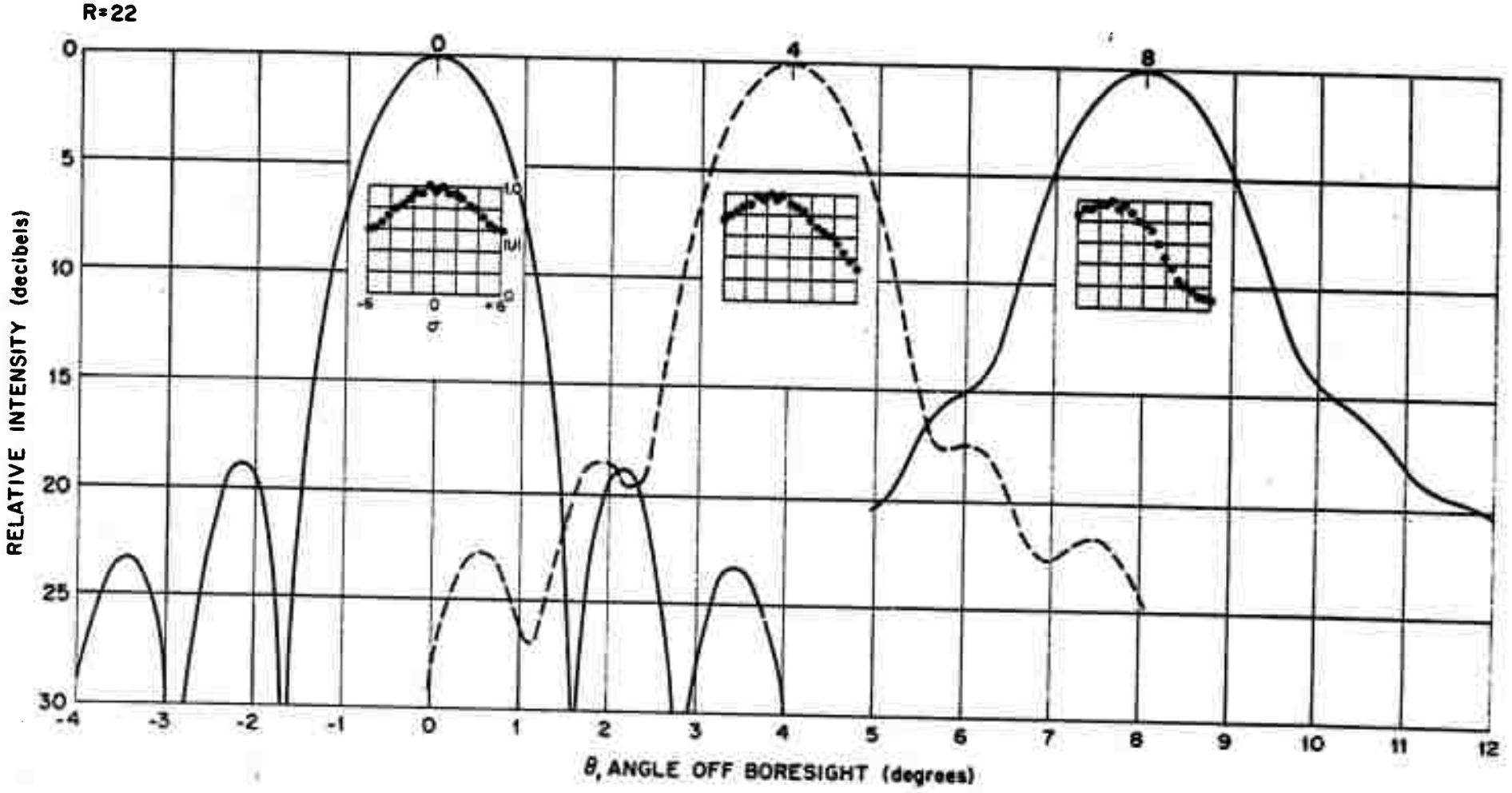

Figure 4: R = 22λ

C-13662-5

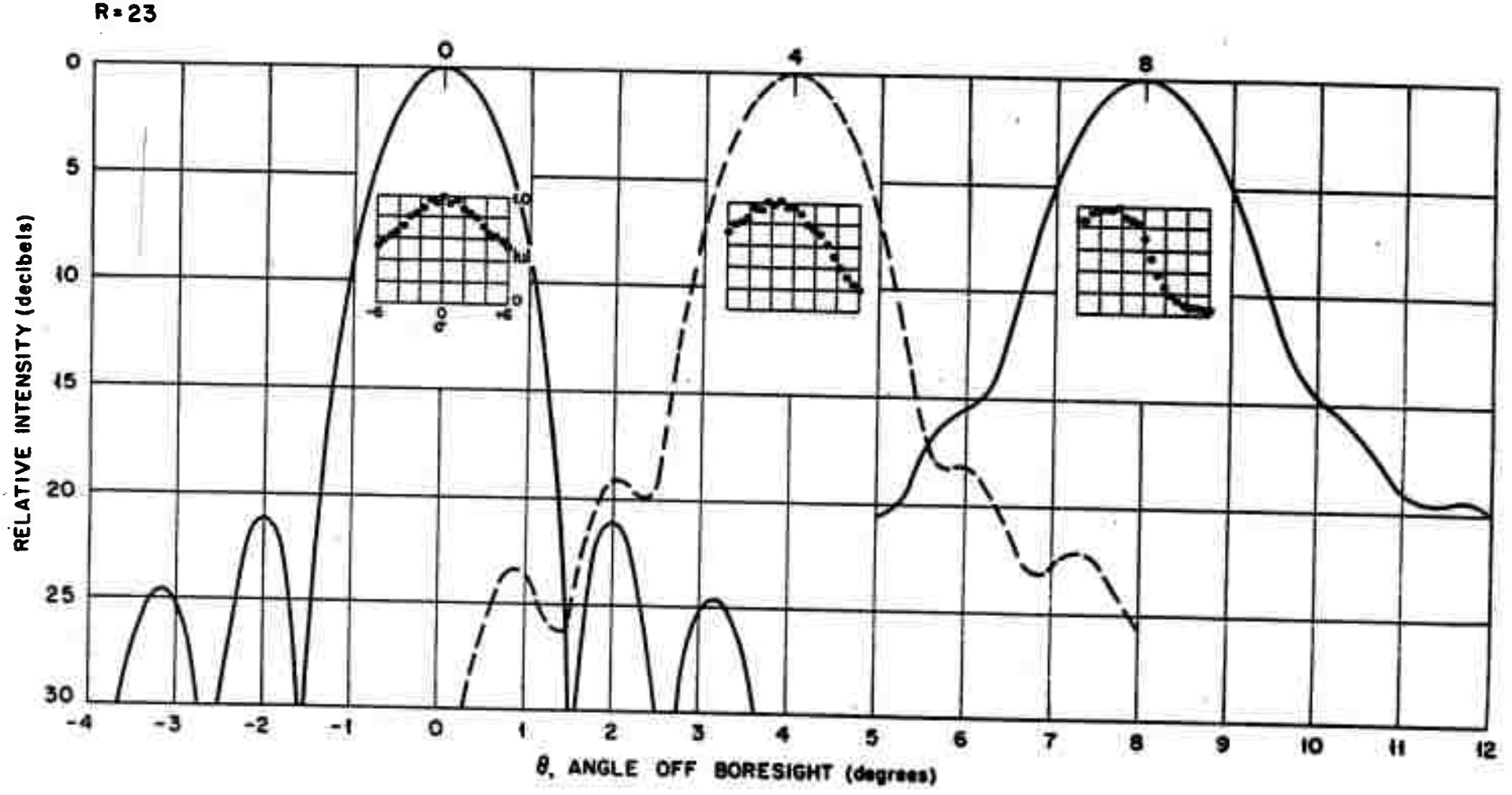

Figure 5: · R = 23λ

C-13662-7

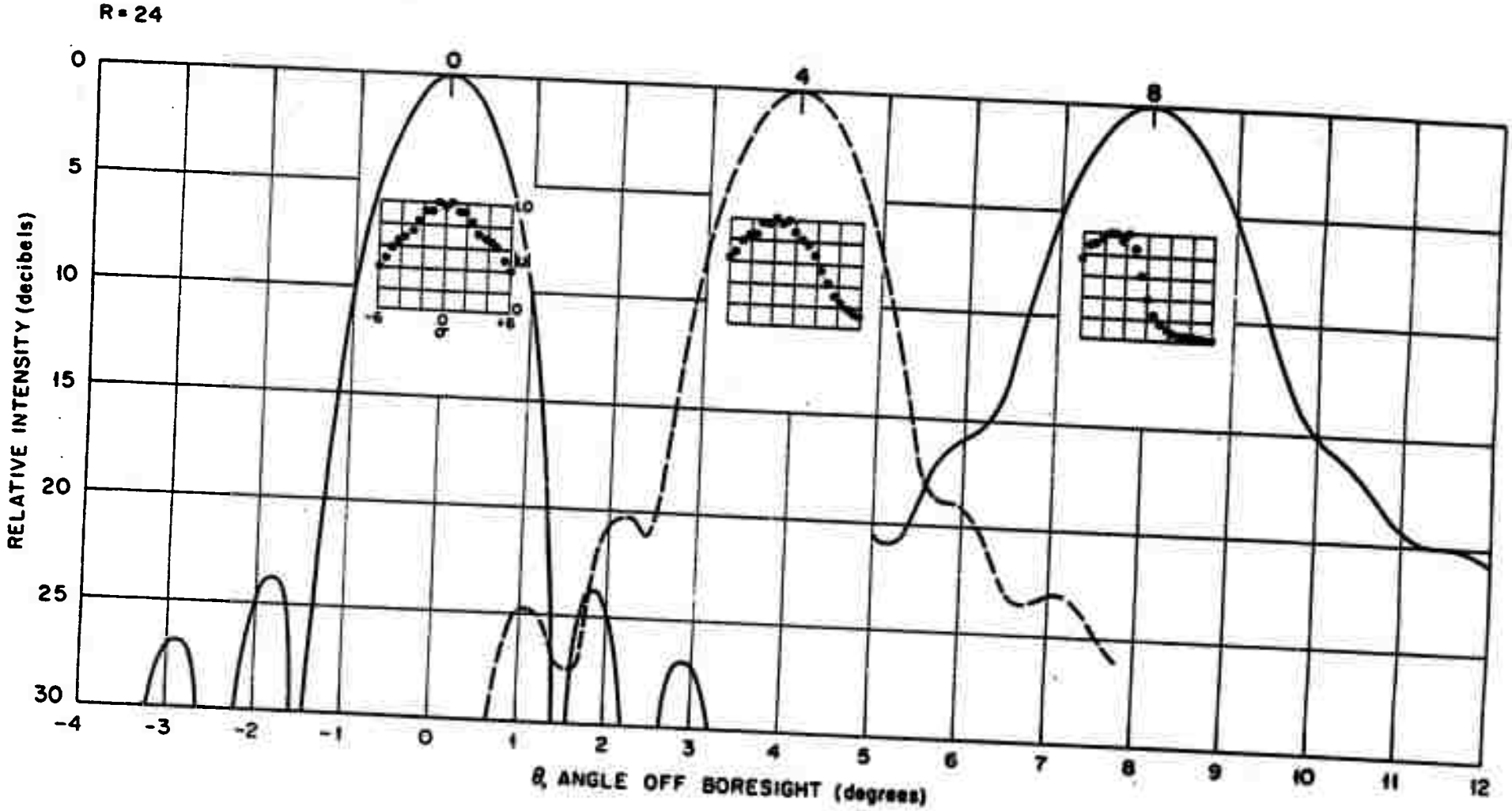

Figure 6: R = 24

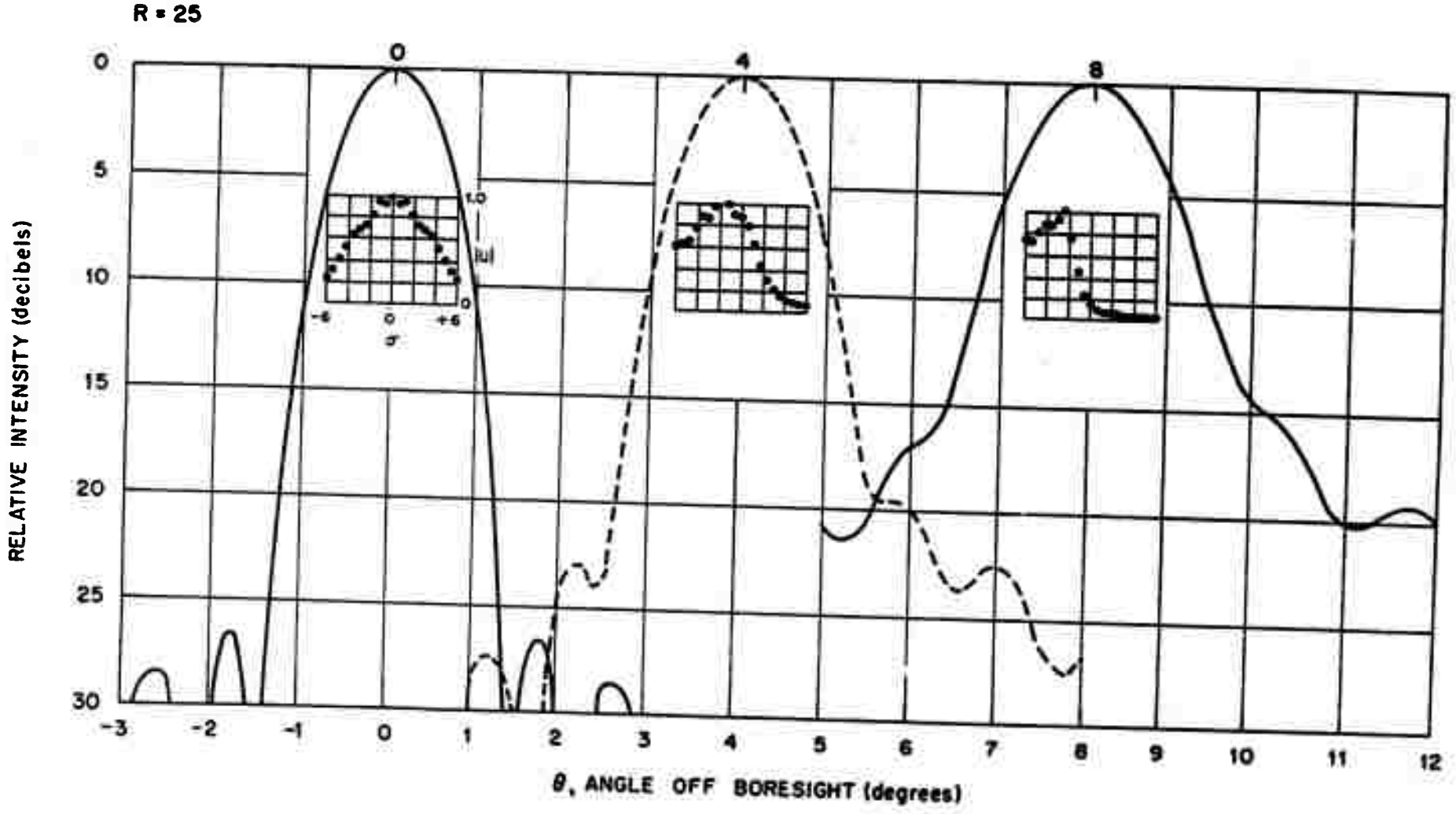

Figure 7: R = 25λ

C-19662

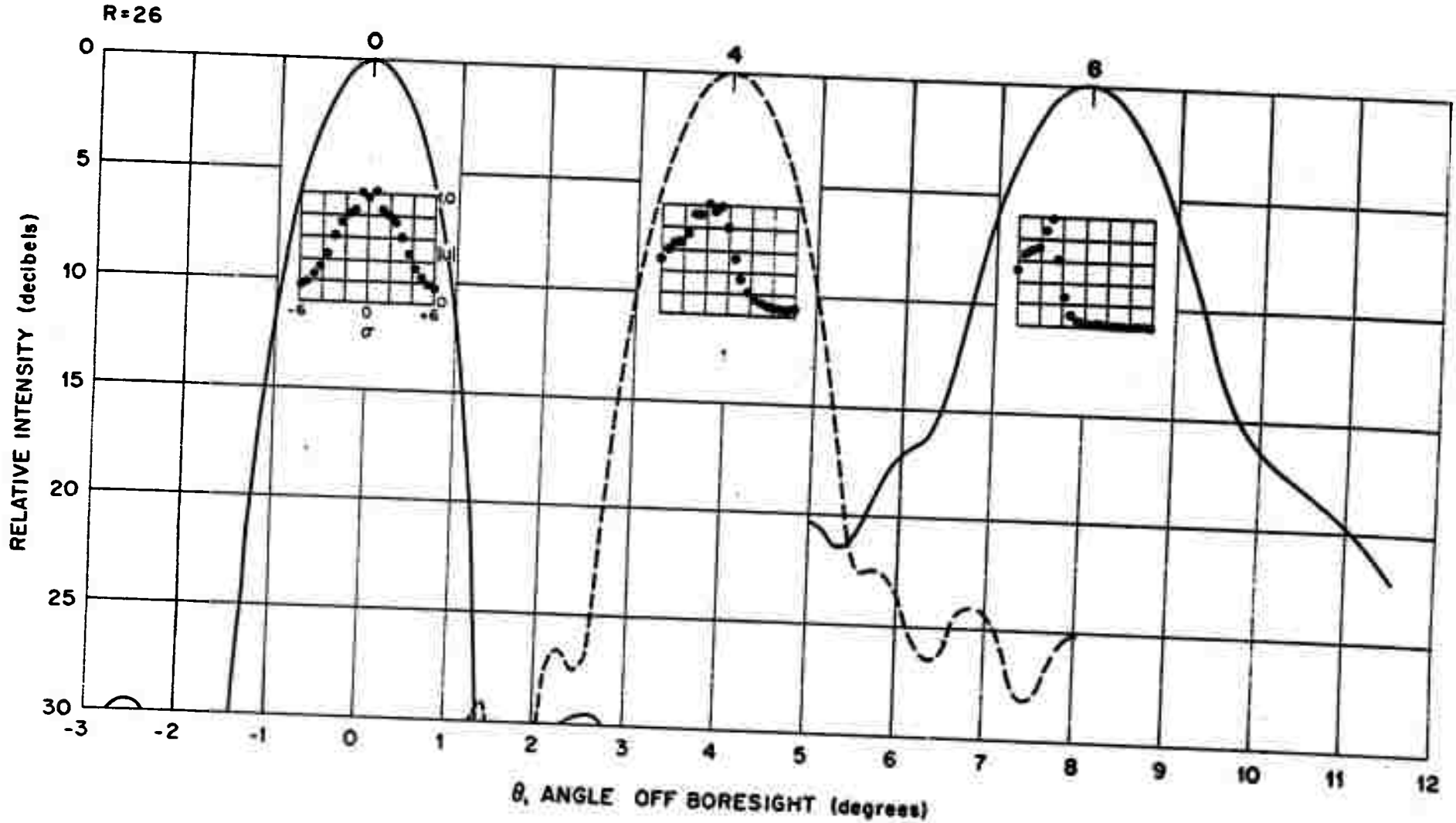

Figure 8: R = 26λ

Figure 9: R = 27λ

A-13662-17

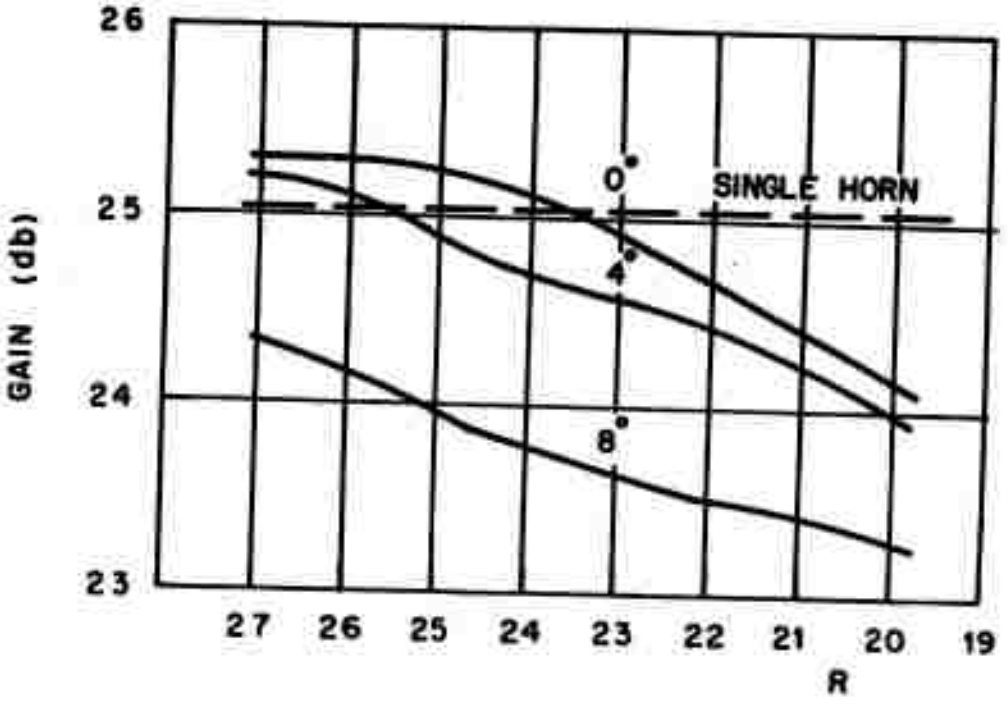

Figure 10: The calculated gain as a function of R. The dashed line is the value that a single horn located at the focus would have.

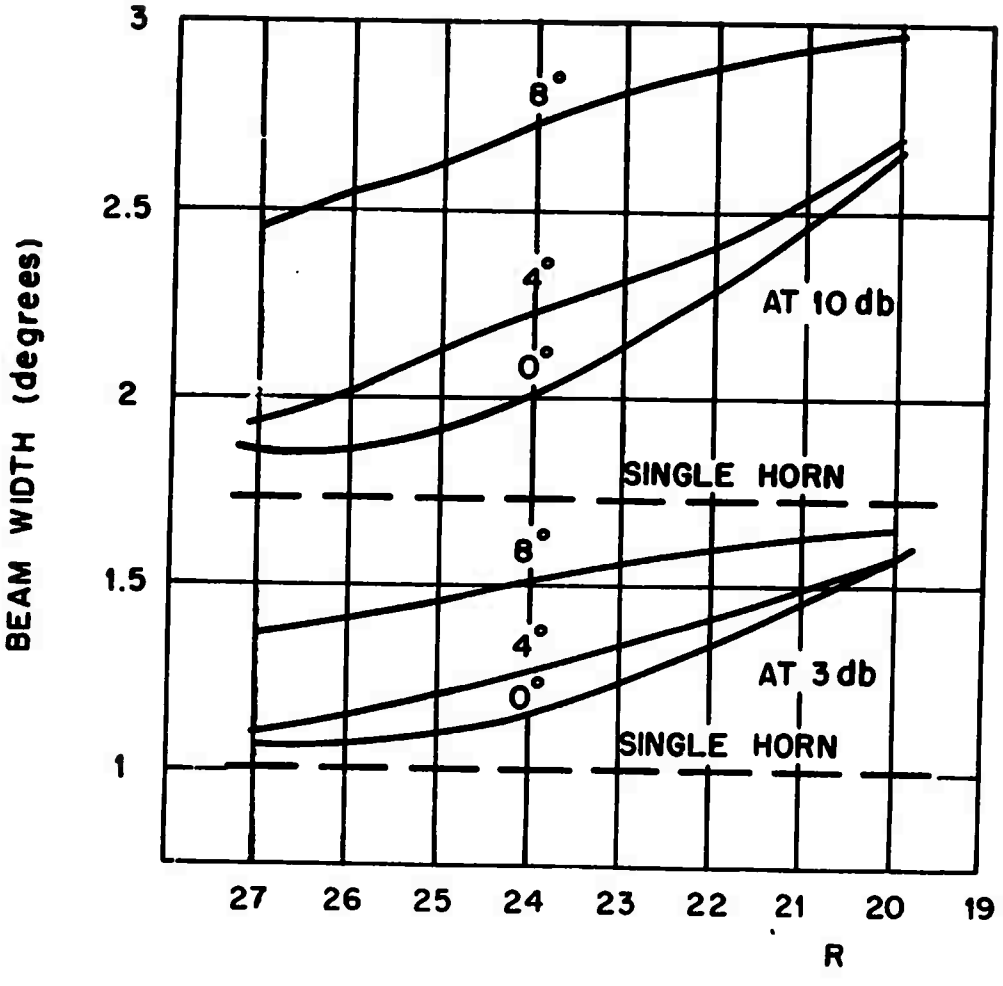

Figure 11: The beamwidth at the 3 db and 10 db levels.

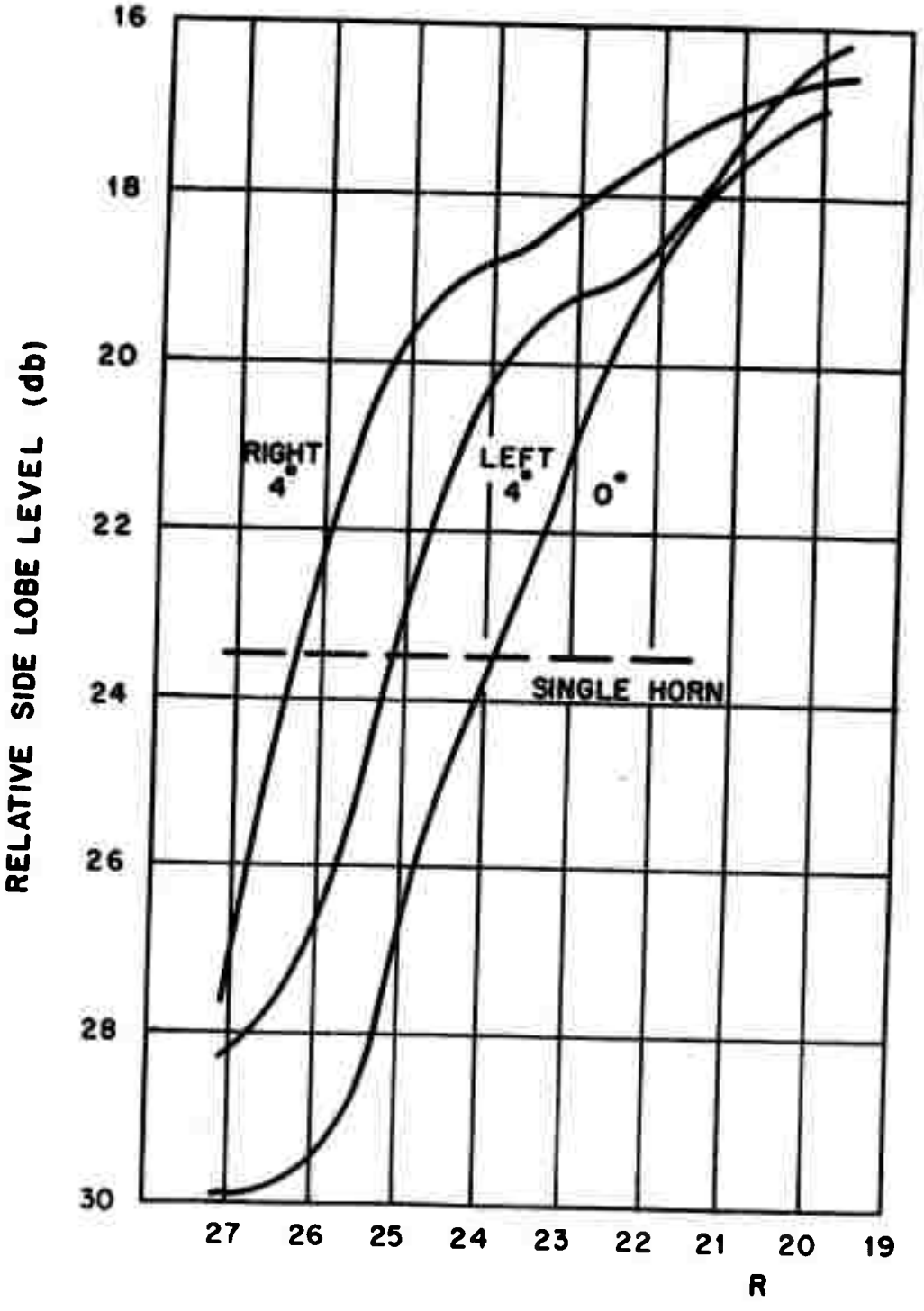

Figure 12: The side lobe level of the highest left and right side lobes.

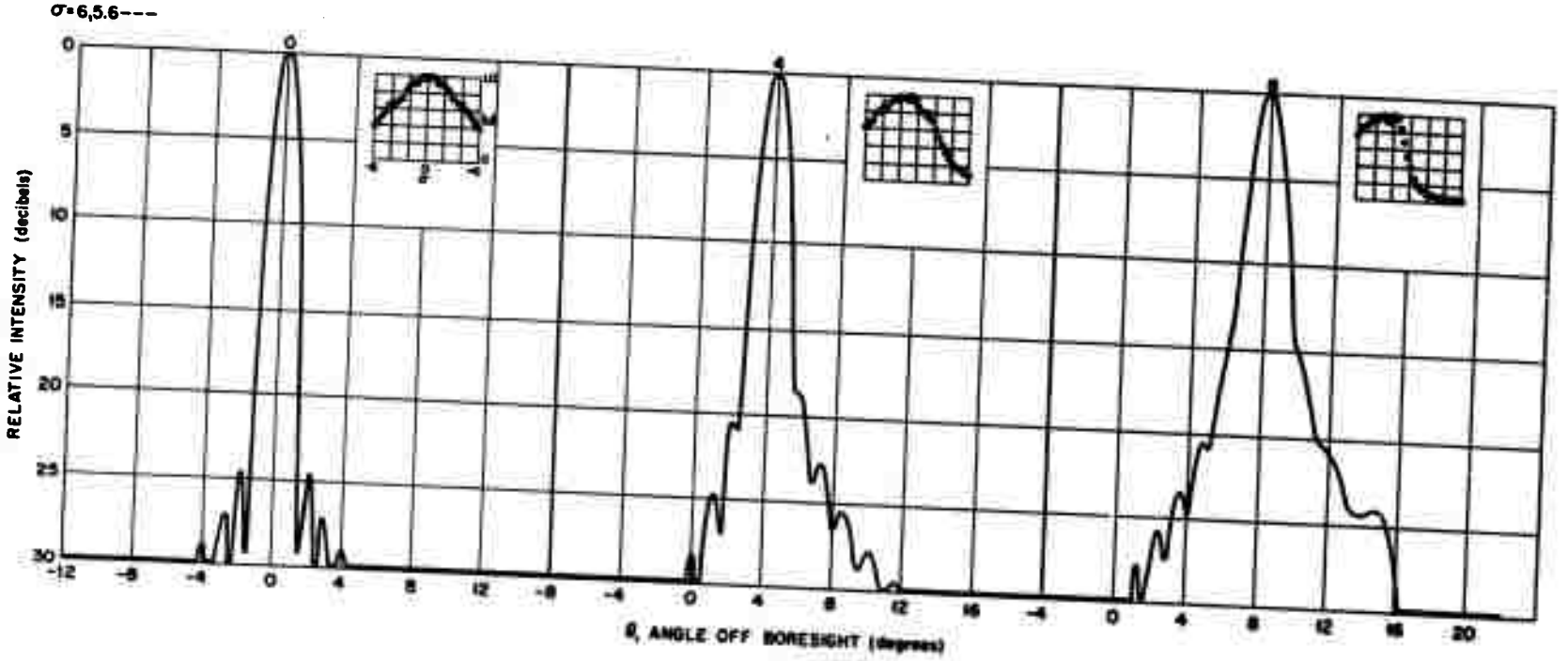

Figure 13: The far-field patterns calculated for R = 24λ, Θ_o = 0°, 4° and 8°. 31 horns separated .4λ, σ = -6.0λ, -5.6λ, -5.2λ ---- +6.0λ. Each pattern has a graph insert showing the horn position σ and horn relative signal amplitude |u|.

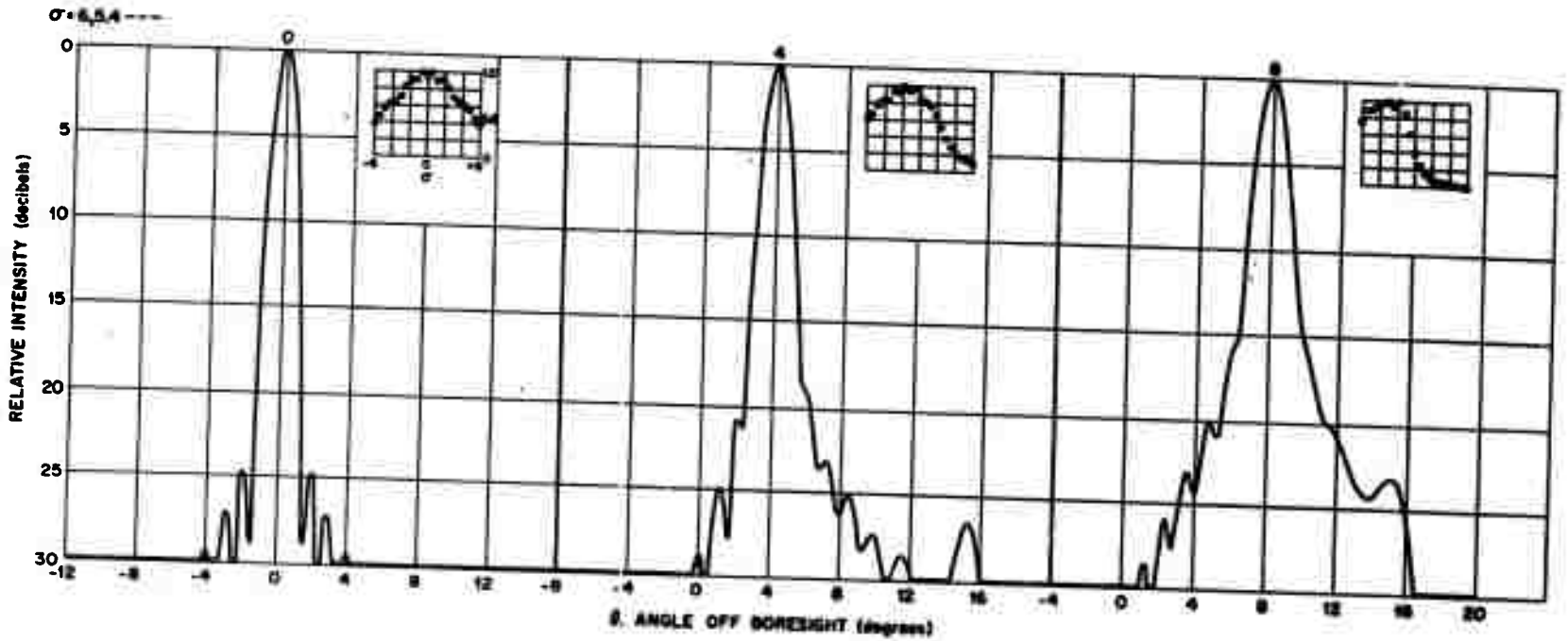

Figure 14: 21 horns separated .6λ, σ = -6.0λ, -5.4λ, -4.8λ ---- +6.0λ.

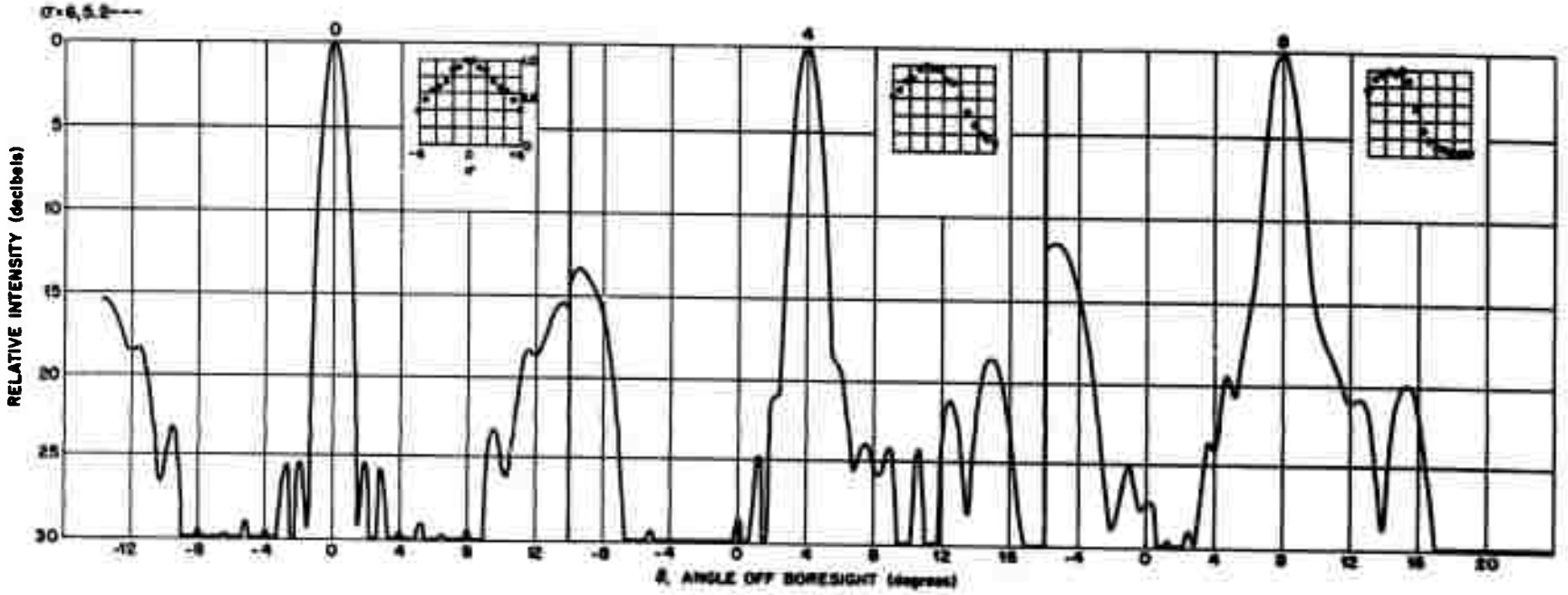

Figure 15: 16 horns separated .8λ, σ = -6.0λ, -5.2λ, -4.4λ ---- +6.0λ.

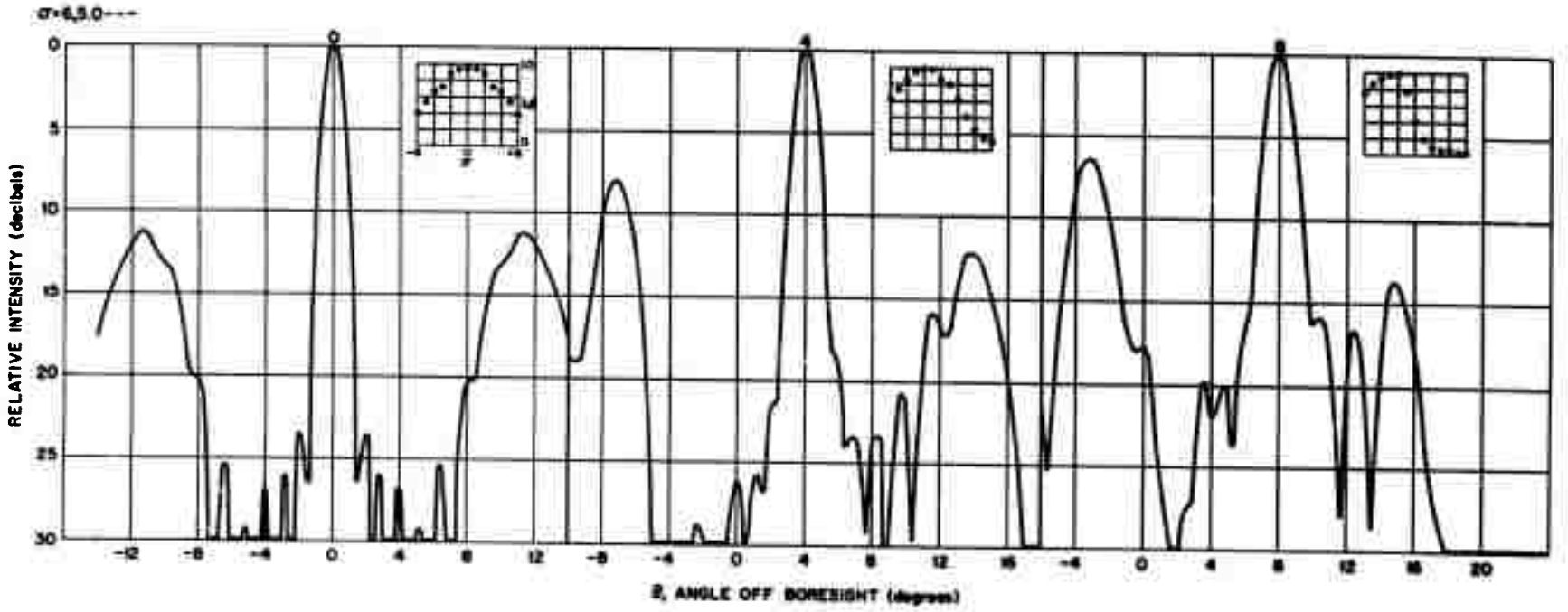

Figure 16: 13 horns separated 1.0λ, σ = -6.0λ, -5.0λ, -4.0λ ---- +6.0λ.

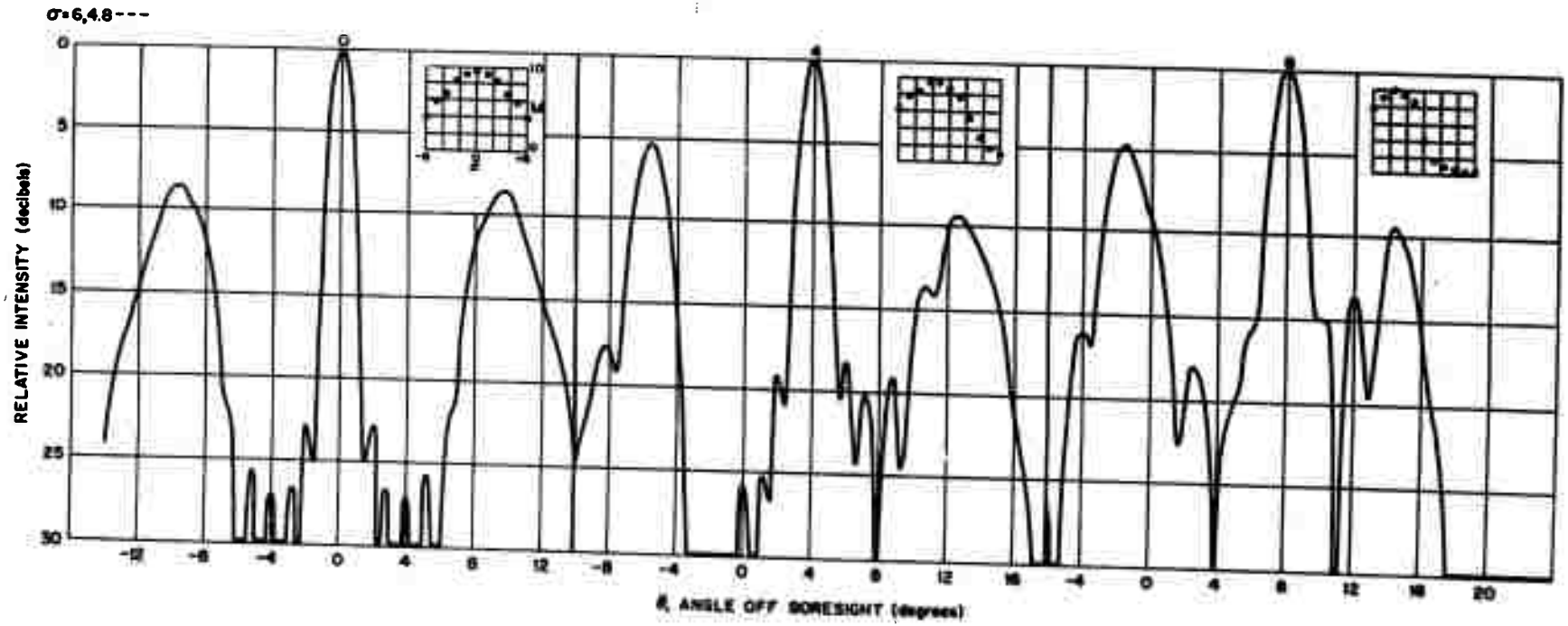

Figure 17: 11 horns separated 1.2λ, σ = -6.0λ, -4.8λ, -3.6λ ---- +6.0λ.

DISTRIBUTION LIST

J. L. Allen
R. N. Assaly
W. W. Camp
W. C. Danforth, Jr.
M. E. Devane
A. R. Dion
J. Freedman
J. V. Harrington
K. J. Keeping
B. F. LaPage
C. A. Lindberg
M. A. Malone
W. E. Morrow
J. B. Resnick
T. F. Rogers
C. B. Slade
P. Waldron
W. W. Ward
H. G. Weiss